3D RESOLUTION MEASURE FOR MULTIFOCAL PLANE MICROSCOPY

Jerry Chao[1,2], Sripad Ram[2], E. Sally Ward[2] and Raimund J. Ober[1,2]*

[1]Department of Electrical Engineering, University of Texas at Dallas, Richardson, TX,
[2]Department of Immunology, University of Texas Southwestern Medical Center, Dallas, TX.

ABSTRACT

The distance separating two biomolecules in close proximity is an important determinant of the nature of their interaction. While much focus has been given to resolving distances in 2D, the 3D cell in which biological interactions occur necessitates the evaluation of resolution in 3D. Recently, we introduced an information-theoretic 3D resolution measure which predicts that the resolution of an optical microscope is unlimited, and that it improves as more photons are detected from the imaged molecules. Here, we investigate the 3D resolution measure for a multifocal plane microscope. Used for the simultaneous imaging of distinct focal planes within a specimen, multifocal plane microscopy has important applications in the tracking of microscopic objects in 3D. By comparing their 3D resolution measures, we determine the circumstances under which a two-plane microscope setup offers better resolvability than a comparable conventional microscope.

Index Terms— Resolution measure, Fisher information matrix, Cramer-Rao inequality, multifocal plane microscopy

1. INTRODUCTION

The ability to determine the distance separating two closely spaced biomolecules is of importance in assessing the nature of their interaction. With imaging of biological interactions at the level of individual biomolecules made possible by single molecule microscopy, it is of practical interest to characterize an imaged interaction by resolving the distance separating the two participants.

While much work has concentrated on resolving separation distances in a 2D context, there is a need to consider the resolution problem in 3D since biological interactions take place inside a 3D cellular environment. In the 2D context, the resolution limit imposed by Rayleigh's criterion is widely believed to be an impediment to the study of biological interactions, which typically take place at nanometer scale separation distances. Recently, a 2D resolution measure based on information theory was presented which shows that Rayleigh's resolution limit can be overcome [1]. In fact, this resolution measure predicts that the resolution of an optical microscope

is unlimited, and that it can be improved by detecting more photons from the imaged molecule pair. Therefore, instead of addressing whether a given separation distance is resolvable by a particular imaging setup, the resolution measure tells us with what accuracy a given separation distance can be resolved. Based on the same theoretical framework, an analogous result was subsequently derived for the 3D context [2]. The proposed 3D resolution measure gives a lower bound on the accuracy with which the distance between two single molecules situated in 3D space can be determined. This 3D resolution measure is readily applicable to a conventional single focal plane microscope setup.

Multifocal plane microscopy [3] is a technique that allows the simultaneous imaging of multiple focal planes within a specimen. It has important applications in determining the 3D location of a single molecule [4] and in visualizing the path traversed by a microscopic object in 3D space [5]. Here, we present the 3D resolution measure for a multifocal plane microscope setup. We consider its dependence on the number of photons collected from the single molecule pair, the axial location of the single molecular pair, and the distance separating the two molecules. Importantly, we compare the resolution measures for a two-plane setup and a conventional single focal plane microscope, and we identify the circumstances under which improved resolvability is obtained with the two-plane setup. For additional studies on the two-plane resolution measure and its comparison with the conventional single-plane resolution measure, see [6].

2. MULTIFOCAL PLANE MICROSCOPY

The principle of multifocal plane microscopy [3] is illustrated in Fig. 1. In the conventional single-plane microscope setup, the camera is positioned at detector plane 1 and captures images of the specimen at focal plane 1. Detector plane 1 can, for example, be the infinity-corrected detector plane, and focal plane 1 the infinity-corrected standard focal plane. In a two-plane setup, a second camera is situated at a detector plane 2 that is distinct from detector plane 1. This second camera accordingly captures images of the specimen at a focal plane 2 that is distinct from focal plane 1. If detector plane 2 is closer to the microscope optics than detector plane 1 as shown in Fig. 1, then its corresponding focal plane 2 is fur-
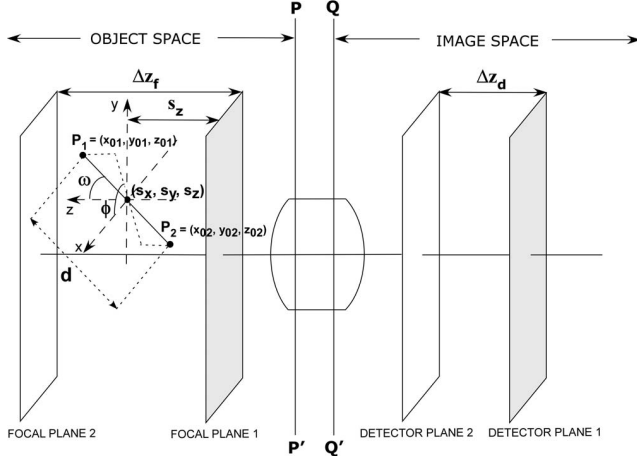
Fig. 1. Principle of multifocal plane microscopy. The schematic shows two detector planes positioned at different distances from the microscope lens system, each of which images a distinct focal plane in the object space. Also depicted is a pair of molecules separated by a distance d and joined by a line segment P_1P_2 with midpoint (s_x, s_y, s_z) and orientation angles ω and ϕ.

ther from the optics than focal plane 1. By splitting the fluorescence collected by the objective into two light paths with a beam splitter, the two cameras can image simultaneously their respective focal planes within the specimen. For a schematic of a physical realization of a two-plane setup, see [4].

3. 3D RESOLUTION MEASURE

The task of determining the distance separating two single molecules is formulated as a parameter estimation problem in which the unknown parameter to be estimated from the acquired image data is the distance d that separates the two single molecules. The 3D resolution measure is defined as the square root of the inverse of the Fisher information matrix $\mathbf{I}(d)$ calculated for this estimation problem. By the Cramer-Rao inequality $Var(\hat{d}) \geq \mathbf{I}^{-1}(d)$, the 3D resolution measure as defined provides a lower bound on the accuracy of the estimates of d by any unbiased estimator $\hat{d}$. The underlying approach for the derivation of the 3D resolution measure for a single focal plane can be found in [1, 7]. Here we give a brief description that leads to an expression for the 3D resolution measure for a two-plane imaging setup.

For a general parameter estimation problem in optical microscopy, the acquisition of image data is modeled as a spatio-temporal random process which we refer to as the image detection process [7]. For a scalar unknown parameter $\theta \in \Theta$, Θ being the parameter space, the Fisher information matrix for image data captured by a pixelated detector during the time interval $[t_0, t]$ is given by

$$\mathbf{I}(\theta) = \sum_{k=1}^{N_p} \frac{1}{\mu_\theta(k,t)+\beta(k,t)} \left(\frac{\partial \mu_\theta(k,t)}{\partial \theta} \right)^2,$$

where $\mu_\theta(k, t) = \int_{t_0}^{t} \int_{C_k} \Lambda(\tau) f_{\theta,\tau}(r) dr d\tau$ is the mean of the Poisson-distributed number of photons from the single molecules detected at the kth pixel C_k, $\beta(k, t)$ is the mean of the Poisson-distributed number of spurious photons at pixel C_k due to noise sources such as cellular autofluorescence and scattering, and N_p is the number of pixels. In the expression for μ_θ, Λ denotes the intensity function of the inhomogeneous Poisson process which models the time points at which photons are detected, and it is assumed to be independent of the unknown parameter θ. The term $f_{\theta,\tau}$ denotes the density function of the independent random variables that model the spatial coordinates at which the photons hit the detector.

If noise introduced by the detector readout process is to be accounted for, then the expression for the Fisher information matrix becomes more complex, and is given in [6].

For the 3D resolution problem, we have $\theta = d$, and the intensity function is given by $\Lambda(\tau) = \Lambda_1(\tau) + \Lambda_2(\tau), \tau \geq t_0$, where Λ_1 and Λ_2 are the photon detection rates of the two single molecules. The density function is given by

$f_{d,\tau}(r) = \frac{\epsilon_1(\tau)}{M^2} q_{z_{01}(d),1} \left(\frac{x}{M} - x_{01}(d), \frac{y}{M} - y_{01}(d) \right) + \frac{\epsilon_2(\tau)}{M^2} q_{z_{02}(d),2} \left(\frac{x}{M} - x_{02}(d), \frac{y}{M} - y_{02}(d) \right),$

where $r = (x, y) \in \mathbb{R}^2$, $\epsilon_i(\tau) = \Lambda_i(\tau)/(\Lambda_1(\tau) + \Lambda_2(\tau))$, $i = 1, 2$, $\tau \geq t_0$, (x_{01}, y_{01}, z_{01}) and (x_{02}, y_{02}, z_{02}) are the 3D spatial coordinates of the two single molecules, M denotes the magnification of the imaging setup, and $q_{z_{01}(d),1}$ and $q_{z_{02}(d),2}$ denote the image functions of the two single molecules. An image function q_{z_0} is defined as the image of an object at unit magnification when the object is located at $(0, 0, z_0)$, $z_0 \in \mathbb{R}$, in the object space [7]. As shown in Fig. 1, the coordinates of each single molecule can be expressed as functions of the separation distance d, and in terms of the coordinates (s_x, s_y, s_z) of the midpoint of the line segment P_1P_2 joining the two single molecules and the orientation angles ω and ϕ of P_1P_2. For a conventional imaging setup consisting of just focal plane 1, the 3D resolution measure is the square root of the inverse of the Fisher information matrix we have described thus far.

In a multifocal plane imaging setup, the data acquired from each focal plane is described by an independent image detection process, and the Fisher information matrix for the entire setup is just the sum of the Fisher information matrices for data acquired from the individual focal planes. The Fisher information matrix $\mathbf{I}_{tot}(d)$ for a two-plane setup is therefore $\mathbf{I}_{tot}(d) = \mathbf{I}_{plane1}(d) + \mathbf{I}_{plane2}(d)$, where $\mathbf{I}_{plane1}(d)$ and $\mathbf{I}_{plane2}(d)$ are the Fisher information matrices for data acquired from the two focal planes. The expression for $\mathbf{I}_{plane2}(d)$ is identical to that for $\mathbf{I}_{plane1}(d)$, except in two respects. First, the axial coordinates $z_{01}(d)$ and $z_{02}(d)$ of the two molecules are specified with respect to focal plane 2. Second, the magnification is different for focal plane 2. By definition, the 3D resolution measure for a two-plane setup is just the square root of $\mathbf{I}_{tot}^{-1}(d)$.

4. RESULTS

For all calculations, a specific imaging setup is considered with a specific set of experimental conditions. The presented results are accordingly specific to the assumed setup and conditions. It should be noted, however, that the general nature of our theoretical framework allows the same type of calculations to be performed for different imaging setups and experimental conditions.

We assume the two single molecules to have equal intensity and a constant photon detection rate, i.e., $\Lambda_1(\tau) = \Lambda_2(\tau) = \Lambda_0$, $\tau \geq t_0$, where Λ_0 is a constant. Furthermore, we assume the two single molecules to have the same image function q_{z_0}, i.e., $q_{z_0}(x, y) = q_{z_0,1}(x, y) = q_{z_0,2}(x, y)$, $(x, y) \in \mathbb{R}^2$, $z_0 \in \mathbb{R}$, given by the scalar diffraction-based 3D point spread function [8]

$$q_{z_0}(x,y) = \frac{\left| \int_0^1 J_0 \left(ka\rho \frac{\sqrt{x^2+y^2}}{z_d} \right) e^{jW_{z_0}(\rho)} \rho d\rho \right|^2}{\int_{\mathbb{R}^2} \left| \int_0^1 J_0 \left(ka\rho \frac{\sqrt{x^2+y^2}}{z_d} \right) e^{jW_{z_0}(\rho)} \rho d\rho \right|^2 dxdy}, \quad (1)$$

where (x, y) denotes an arbitrary point on the detector plane, z_d denotes the axial distance of the detector plane from the back focal plane of the microscope lens system, $k = 2\pi/\lambda$, λ being the wavelength of the detected photons, a denotes the radius of the limiting aperture of the microscope projected onto the back focal plane of the lens system, J_0 denotes the zeroth order Bessel function of the first kind, and W_{z_0} denotes the phase aberration term. The phase aberration is given by $W_{z_0}(\rho) = \frac{\pi(NA)^2 z_0}{n_{oil}\lambda} \rho^2$, $\rho \in (0, 1)$, $z_0 \in \mathbb{R}$, where NA is the numerical aperture of the objective and n_{oil} is the refractive index of the immersion oil. The function W_{z_0} as defined corresponds to the classical 3D point spread function model of Born and Wolf [9].

All results computed for the two-plane microscope setup assume a focal plane spacing of $\Delta z_f = 500$ nm (see Fig. 1), a value which we have used in an actual setup. The magnification for focal plane 1 is set to 100, and that for focal plane 2, based on the 500 nm plane spacing, is determined to be 97.98 using geometrical optics. The two single molecules are assumed to lie in the xz plane, i.e., the angle $\phi = 0$, at a 45° angle from the positive z axis, i.e., the angle $\omega = \pi/4$, and the midpoint of the line segment joining them is taken to be the center of a 21×21 pixel array with a pixel size of 13 μm $\times$ 13 μm. The photon detection rate is set to $\Lambda_0 = 2500$ photons/s per single molecule per focal plane. The wavelength is set to $\lambda = 520$ nm, the image acquisition time is set to $t = 1$ s (with $t_0 = 0$ s), the numerical aperture of the objective is set to $NA = 1.45$, and the refractive index of the immersion oil is set to $n_{oil} = 1.515$. For each focal plane, the mean of the additive Poisson noise (e.g., cellular autofluorescence, scattering), if present, is set to 80 photons/pixel/s for all pixels.

For comparison, the conventional single-plane imaging setup is taken to be one that consists of only focal plane 1. Since in the two-plane setup the total fluorescence is assumed to be split equally into two light paths, the photon detection rate is doubled in the single-plane setup to 5000 photons/s per single molecule. Similarly, the mean of the additive Poisson noise, if present, is doubled to 160 photons/pixel/s for all pixels.

When detector readout noise is considered, for any focal plane the mean and standard deviation of the additive Gaussian noise are set to 0 e$^-$ per pixel and 8 e$^-$ per pixel, respectively, for all pixels.

Dependence on photon count Fig. 2 shows, for four different separation distances d, the dependence of the two-plane 3D resolution measure on the expected number of detected photons per single molecule. The curves show that the accuracy in determining a given separation distance can be improved by collecting more photons from each single molecule. For example, for a photon count of 2500 per molecule, the resolution measure predicts an accuracy of ± 25.7 nm to resolve a distance of 20 nm. However, if the photon count is increased to 30000 per molecule, then the predicted accuracy is improved to ± 7.4 nm.

Dependence on axial location For four different separation distances d between the two single molecules, Fig. 3 shows the 3D resolution measure for the two-plane setup as a function of the axial distance s_z (see Fig. 1) of the single molecule pair from focal plane 1. For all four values of d, the resolution measure exhibits a symmetry about the midpoint between the two focal planes, i.e., about $s_z = \Delta z_f/2 = 250$ nm. It is important to note, however, that due to the difference in the magnification for the two focal planes, this symmetry is only approximate. Also for all four values of d, the resolution measure remains relatively flat in the one-micron interval centered about the midpoint between the two focal planes (i.e., from $s_z = -250$ nm to $s_z = 750$ nm), outside of which the resolution measure undergoes a more pronounced deterioration. Therefore, the best accuracy is predicted for resolving the separation distance when the center of the single molecule pair is axially within half a plane spacing from either focal plane.

Dependence on separation distance For a given axial location s_z of the single molecule pair, Fig. 3 shows that the resolution measure consistently deteriorates as the separation distance d decreases. That is, the closer the two molecules are to each other, the less accurately we are able to determine the distance between them. For example, in the flat one-micron interval, the resolution measure predicts an accuracy in the range of ± 4.8 nm to ± 6.7 nm (± 13.3 nm to ± 18.0 nm) to resolve a separation distance of 200 nm (50 nm). On the other hand, poor accuracy in the range of ± 32.4 nm to ± 43.9 nm (± 64.5 nm to ± 87.4 nm) is predicted for resolving a separation distance of 20 nm (10 nm).

Conventional single-plane setup vs. two-plane setup Fig. 4 gives a comparison of the 3D resolution measure for the two-plane setup with that for the corresponding conventional single-plane setup. Plots are shown for separation distances of 20 nm and 50 nm. Note that for either separation dis-
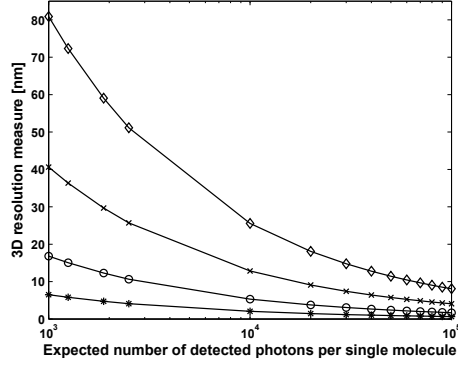
Fig. 2. Dependence of two-plane 3D resolution measure on the detected photon count for a pixelated detector in the absence of noise sources, shown for separation distances $d = 10$ nm ($\diamond$), $d = 20$ nm ($\times$), $d = 50$ nm ($\circ$), and $d = 200$ nm ($*$).

Fig. 4. Comparison of conventional and two-plane 3D resolution measures for pixelated detectors in the presence of additive Poisson and Gaussian noise for separation distances of $d = 20$ nm ($\times$ single-plane, $\diamond$ two-plane) and $d = 50$ nm ($*$ single-plane, $\circ$ two-plane).
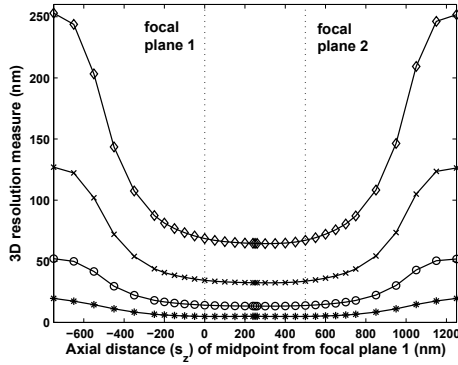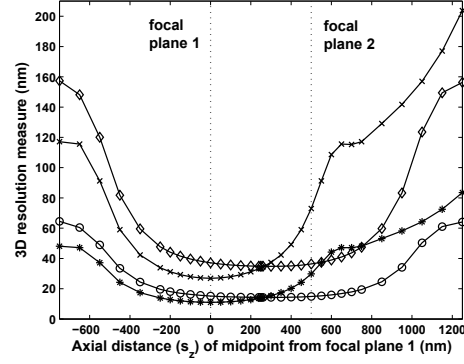

Fig. 3. Two-plane 3D resolution measure for a pixelated detector in the presence of additive Poisson noise for separation distances of $d = 10$ nm ($\diamond$), $d = 20$ nm ($\times$), $d = 50$ nm ($\circ$), and $d = 200$ nm ($*$).

tance, the single-plane resolution measure is symmetric about $s_z = 0$, which corresponds to the axial location of focal plane 1. For both separation distances, the plots show that better resolution is obtained with the two-plane setup when the single molecule pair is situated closer to focal plane 2 (i.e., roughly when $s_z > \Delta z_f/2 = 250$ nm). In other words, advantage is gained with the introduction of a second focal plane only when the imaged single molecule pair sits closer to the added plane. In particular, significant advantage is gained with the two-plane setup in the interval from $s_z = 250$ nm to $s_z = 750$ nm. In that interval, a separation distance of 50 nm (20 nm) is predicted to be resolvable with the two-plane setup with an accuracy ranging from ±14.3 nm to ±19.5 nm (±34.8 nm to ±47.4 nm), compared to ±13.9 nm to ±48.1 nm (±33.8 nm to ±117.2 nm) with the single-plane setup.

5. REFERENCES

[1] S. Ram et. al., "Beyond Rayleigh's criterion: A resolution measure with application to single-molecule microscopy," *PNAS*, vol. 103, no. 12, pp. 4457–4462, 2006.

[2] S. Ram et. al., "A novel 3D resolution measure for optical microscopes with applications to single molecule imaging," *Proc. of SPIE*, vol. 6444, no. 64440D, 2007.

[3] P. Prabhat et. al., "Simultaneous imaging of different focal planes in fluorescence microscopy for the study of cellular dynamics in three dimensions," *IEEE Trans. Nanobioscience*, vol. 3, pp. 237–242, 2004.

[4] S. Ram et. al., "A novel approach to determining the three-dimensional location of microscopic objects with applications to 3D particle tracking," *Proc. of SPIE*, vol. 6443, no. 64430D, 2007.

[5] P. Prabhat et. al., "Elucidation of intracellular recycling pathways leading to exocytosis of the Fc receptor, FcRn, by using multifocal plane microscopy," *PNAS*, vol. 104, pp. 5889–5894, 2007.

[6] J. Chao et. al., "Resolution in 3D in multifocal plane microscopy," *Proc. of SPIE*, vol. 6861, no. 68610Q, 2008.

[7] S. Ram et. al., "A stochastic analysis of performance limits for optical microscopes," *Multidim. Syst. Sig. Process.*, vol. 17, pp. 27–57, 2006.

[8] S. F. F. Gibson, *Modeling the 3D imaging properties of the fluorescence light microscope*, Ph.D. thesis, Carnegie-Mellon University, 1990.

[9] M. Born and E. Wolf, *Principles of Optics*, Cambridge University Press, Cambridge, UK, 1999.